Anisotropic Spin-Lattice Relaxation Rates of Some Rare-Earth-Doped Lanthanum Trichlorides*†

R. C. MIKKELSON‡ AND H. J. STAPLETON§
Department of Physics and Materials Research Laboratory, University of Illinois, Urbana, Illinois

We have measured the temperature dependence and the angular anisotropy of the spin-lattice relaxation rate $1/T_1$ of cerium, praseodymium, neodymium, samarium, terbium, and erbium in single crystals of anhydrous lanthanum trichloride. The experiments were performed at X-band frequencies using pulse-saturation techniques on samples containing ≤ 2 at.% rare-earth doping for temperatures between 1.65 and 4.2°K. Angular measurements at constant temperature were made for magnetic-field orientations between 0° and 90° with respect to the crystal c axis. The results are interpreted as involving an angular-dependent direct process and isotropic Orbach and Raman mechanisms. These results are compared with theoretically predicted rates obtained from our computer calculations, which are based upon Orbach's approach and require a knowledge of the static crystal-field parameters. Since rare-earth trichlorides have been the object of much optical investigation, these parameters are available for all ions we treat except cerium. Except for this ion, most of the predicted relaxation rates agree with experiments to within a factor of 5 or less, and for all ions the form of the angular anistropy is followed almost exactly. Theoretical treatments which involve the mixing of excited-state wave functions into the ground magnetic doublet through the anisotropic Zeeman interaction are required to explain the observed angular dependence. One of the ions, praseodymium, exhibits a phonon-limited direct-process relaxation rate which is interesting because the apparent hot-phonon equilibration time is about 80 nsec and corresponds to an equilibration path length of only 160 μ. After neutron bombardment the bottlenecked relaxation rate changed and the equilibration time was apparently reduced to 53 nsec. Prior irradiation of this same sample with 100-keV x rays produced no observable change in the relaxation time. No dependence upon crystal size was observed for the phonon bottleneck in Pr^{3+}-doped $LaCl_3$.

I. INTRODUCTION

THE mechanisms involved in spin-lattice relaxation have received renewed attention recently due in part to their importance for masers, optical linewidths, dynamic nuclear polarization, "hot-phonon" generation, etc. It has been known for many years that the dominant process which brings a spin system into thermal equilibrium is a phonon-induced modulation of the crystalline electrostatic field which interacts with the spins through spin-orbit coupling.[1] Quantitative predictions of relaxation rates based upon point-charge models were generally several orders of magnitude in error, particularly in the liquid-helium temperature region.

Recently, Orbach[2] introduced a phenomenological approach which relies heavily upon a knowledge of experimentally determined static crystal-field parameters and the use of the operator techniques of Elliott and Stevens.[3,4] Experiments at Oxford[5,6] and Berkeley[7,8] on the relaxation rates of rare-earth ethylsulfates and double nitrates indicated remarkable success for Orbach's approach in predicting the observed temperature dependencies of spin-lattice relaxation times in these salts. Various investigators[9–13] subsequently reported varying degrees of agreement when using this technique to predict the temperature-dependent relaxation times of ions from various transition groups in other lattices. It should be noted, however, that frequently these latter calculations were hampered by a lack of sufficient information concerning the static crystalline field surrounding the paramagnetic ion.

In this paper we compare our measurements of the spin-lattice relaxation times of six rare-earth ions substituted into the diamagnetic host lattice, anhydrous lanthanum trichloride, with the calculated values using Orbach's approach as modified by Scott and Jeffries.[7] Particular emphasis is given to the angular dependence of the relaxation time in the temperature range between 1.65 to 4.2°K. The choice of $LaCl_3$ as the host matrix was based upon the extensive knowledge of energy levels and static crystal-field parameters which allow the calculation of wave functions for most of the rare-earth ions in this material. These data are the result of electron-spin-resonance measurements by Hutchison and Wong[14] and optical measurements by various

* Supported in part by the Advanced Research Projects Agency of the U. S. Department of Defense under Contract SD-131 and the Alfred P. Sloan Foundation.

† This paper is based upon a dissertation submitted by R. C. Mikkelson in partial fulfillment of the requirements for the Ph.D. degree at the University of Illinois.

‡ Present address: Physics Department, Macalester College, St. Paul, Minnesota.

§ Alfred P. Sloan Research Fellow.

[1] The reader is referred to Refs. 2 and 7 for the historically important papers.

[2] R. Orbach, Proc. Roy. Soc. (London) **A264**, 458 (1961).

[3] K. W. H. Stevens, Proc. Phys. Soc. (London) **A65**, 209 (1952).

[4] R. J. Elliott and K. W. H. Stevens, Proc. Roy. Soc. (London) **A218**, 553 (1953).

[5] C. B. P. Finn, R. Orbach, and W. P. Wolf, Proc. Phys. Soc. (London) **77**, 261 (1961).

[6] A. H. Cooke, C. B. Finn, B. W. Mangum, and R. L. Orbach, J. Phys. Soc. Japan **17**, Suppl. B-1, 462 (1962).

[7] P. L. Scott and C. D. Jeffries, Phys. Rev. **127**, 32 (1962).

[8] R. H. Ruby, H. Benoit, and C. D. Jeffries, Phys. Rev. **127**, 51 (1962).

[9] R. W. Bierig, M. J. Weber, and S. I. Warshaw, Phys. Rev. **134**, A1504 (1964).

[10] R. Orbach, Phys. Rev. **126**, 1349 (1962).

[11] J. Van den Broek and L. C. Van der Marel, Physica **29**, 948 (1963).

[12] J. Van den Broek and L. C. Van der Marel, Physica **30**, 565 (1964).

[13] L. J. Raubenheimer, E. Boesman, and H. J. Stapleton, Phys. Rev. **137**, A1449 (1965).

[14] C. A. Hutchison, Jr., and E. Y. Wong, J. Chem. Phys. **29**, 754 (1958).

groups.[15] Consequently, the theoretical calculations for the relaxation rates can be made with a minimum of arbitrariness.

Paramagnetic-resonance spectra have been observed for eight trivalent rare-earth ions in $LaCl_3$; our measurements include six of these (Ce, Pr, Nd, Sm, Tb, and Er). Gd and Ho are omitted because the former is an S-state ion and the latter gave signals which were too weak for measurement. Preliminary results for Pr^{3+} and Tb^{3+} were briefly reported earlier.[16] Our experiments were performed using pulse-saturation techniques at ≈ 9 kMc/sec on samples doped with ≤ 2 at. % paramagnetic impurity.

A brief description of the procedures involved in our theoretical calculations is given in Sec. II, with particular attention given to the various means by which a theoretical angular dependence is generated. Section III describes the preparation of samples, the experimental apparatus, and the procedures of data collection and analysis. The experimental and theoretical results of each ion are presented in Sec. IV and a final summary with conclusions is given in Sec. V.

II. THEORY

Trivalent rare-earth ions have electronic configurations equivalent to xenon plus $4f^n$ and exhibit spin-orbit splittings which are an order of magnitude larger than the effects of the static crystal field which can therefore be treated as a perturbation on the eigenfunctions of the spin-orbit interaction. In general, accuracy is not seriously impaired by restricting the perturbation to operate only within the various J manifolds and the result of such a treatment is the partial removal of the $2J+1$ degeneracy of a given J level, and the emergence of a collection of states whose wave functions are linear combinations from the basis $|J,J_z\rangle$. This splitting is illustrated schematically in Fig. 1 (i, ii) in which the energy differences of the crystal field states are labeled Δ_i. Kramers' ions, possessing an odd number of $4f$ electrons, retain at least a two-fold degeneracy due to the time-reversal symmetry of the electrostatic interaction, while non-Kramers' ions are not thus restricted. Naturally the observation of paramagnetic resonance at the lowest temperature requires the lowest lying state to be at least a magnetic doublet or a quasidoublet with an energy splitting in the absence of a magnetic field which is smaller than $h\nu$. Figure 1 (iii) illustrates the further removal of degeneracy when an external magnetic field $\mathbf{H}$ is parallel to the c axis of a hexagonal crystal such as $LaCl_3$. The appropriate eigenfunctions for this orientation of $\mathbf{H}$ are designated $|a\rangle$, $|b\rangle$, $|c\rangle$, etc. The magnetic interaction can be described by a Zeeman

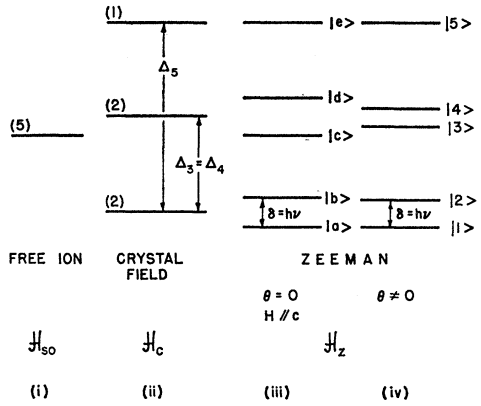

FIG. 1. Schematic energy splittings of the lowest ($J=2$) level of a fictitious rare-earth ion under the combined influence of: (i) the spin-orbit interaction of the free ion; (ii) a crystal field of C_{3h} symmetry; and a Zeeman interaction with the external magnetic field directed (iii) along the crystalline c axis, and (iv) at an angle θ with respect to the crystal axis under the constraint that the magnetic splitting of the ground doublet remain fixed at $h\nu$.

Hamiltonian of the form

$$\mathcal{H}_z=\beta(\mathbf{L}+2\mathbf{S})\cdot\mathbf{H}=\beta\Lambda_J\mathbf{J}\cdot\mathbf{H}, \quad (1)$$

where β is the Bohr magneton and Λ_J is the Lande g factor. The effects of Eq. (1) within a given magnetic doublet can be written in the spin-Hamiltonian formalism as $\beta\mathbf{H}\cdot\mathbf{g}\cdot\mathbf{S}$, where $S=1/2$ and $\mathbf{g}$ is an axially symmetric tensor with principal values $g_\parallel$ and $g_\perp$. States $|1\rangle$ and $|2\rangle$ are just those linear combinations of $|a\rangle$ and $|b\rangle$ which diagonalize the spin Hamiltonian of the ground doublet for an angle θ between $\mathbf{H}$ and the crystal c axis. In a similar manner states $|3\rangle$ and $|4\rangle$ are mixtures of $|c\rangle$ and $|d\rangle$ necessary for the diagonalization of the appropriate spin Hamiltonian of that doublet.

Because of the wealth of optical data available for the trichloride system, the wave functions and crystal-field energy levels of all the ions we have studied are known with the exception of Ce^{3+}. At liquid-helium temperatures only the states $|1\rangle$ and $|2\rangle$ of the ground doublet are populated and at thermal equilibrium the population ratio N_2/N_1 equals $\exp(-\delta/kT)$. If this equilibrium population distribution is disturbed by a pulse of microwaves of energy $h\nu$, this two-level system will return to thermal equilibrium in such a manner that N_2-N_1 approaches its equilibrium value exponentially in time with a mean life T_1.

It can be shown[2,7] that the spin-lattice relaxation rate $1/T_1$ involves three dominant competing processes, each displaying a characteristic temperature dependence. The simplest of these is the direct process involving a spin flip from state $|2\rangle$ to state $|1\rangle$ with the simultaneous emission of a phonon of energy δ. The relaxation rate for this process is given by

$$1/T_{1d}=A(\delta/2k)\coth(\delta/2kT)\approx AT, \quad (2)$$

[15] Specific references to the optical data for each ion are given in Sec. IV.

[16] R. C. Mikkelson and H. J. Stapleton, Bull. Am. Phys. Soc. **10**, 357 (1965).

where

$$A=(3k/\pi\rho v^5)(\delta^2/\hbar^4)|\langle 1|V_c|2\rangle|^2. \quad (3)$$

In this expression for A, the direct process coefficient, ρ is the crystal density, v is a suitably averaged sound velocity for the crystal, and V_c is a dynamic crystal-field Hamiltonian to be discussed later. In our temperature range $(\delta/2kT)\approx 0.1$ so that the direct process should exhibit a relaxation rate directly proportional to the temperature.

A second mechanism, known as the Orbach process, involves the transition of an ion state $|2\rangle$ to state $|i\rangle$ with the energy conserving absorption of a phonon of energy $\Delta_i-\delta/2$ and the subsequent transition from $|i\rangle$ to $|1\rangle$ with the emission of a phonon of energy $\Delta_i+\frac{1}{2}\delta$. The relaxation rate for the Orbach process is given by

$$\frac{1}{T_{10}}=\sum_{i>2}\frac{B_i}{(e^{\Delta_i/kT}-1)}\approx\sum_{i>2}B_i e^{-\Delta_i/kT}, \quad (4)$$

where

$$B_i=\frac{3}{2\pi\rho v^5\hbar}\left(\frac{\Delta_i}{\hbar}\right)^3\frac{2|\langle 1|V_c|i\rangle\langle i|V_c|2\rangle|^2}{|\langle 1|V_c|i\rangle|^2+|\langle i|V_c|2\rangle|^2}. \quad (5)$$

Usually the excited states are well separated so that only the first excited state $|3\rangle$, or $|3\rangle$ and $|4\rangle$ in the case of a doublet, need be considered. Therefore, the Orbach process will usually manifest itself by a simple exponential temperature dependence $\exp(-\Delta_3/kT)$ in the liquid-He temperature region. One necessary requirement for the presence of an Orbach process is that there be phonons available with energy Δ_3, i.e., we require $\Delta_3\lesssim k\Theta_D$, where Θ_D is the Debye temperature.

The third mechanism is the Raman phonon-scattering process where the energy is conserved during the spin transition $|2\rangle$ to $|1\rangle$ by inelastic phonon scattering. The temperature dependence of the Raman process is different for Kramers' and non-Kramers' ions. The Kramers' ions have a relaxation rate

$$1/T_{1R}=C'T^9, \quad (6)$$

where

$$C'=\frac{9!\hbar^2}{\pi^3\rho^2 v^{10}}\left(\frac{k}{\hbar}\right)^9\sum_{i>2}\frac{|\langle 1|V_c|i\rangle\langle i|V_c|2\rangle|^2}{2\Delta_i^4}, \quad (7)$$

and the non-Kramers ions have a relaxation rate

$$1/T_{1R}=(C+C'')T^7, \quad (8)$$

where

$$C+C''=\frac{9\times 6!}{4\pi^3\rho^2 v^{10}}\left(\frac{k}{\hbar}\right)^7\times\left\{|\langle 1|V_c|2\rangle|^2+\sum_{i>2}\frac{|\langle 1|V_c|i\rangle\langle i|V_c|2\rangle|^2}{\Delta_i^2}\right\}. \quad (9)$$

The difference in temperature dependence comes about because of a Van Vleck cancellation in summing over the time conjugate states of Kramers' doublets in the derivation of Eq. (6). There is no term corresponding to C in the Kramers' case because the states $|1\rangle$ and $|2\rangle$ are degenerate under time reversal and the electrostatic interaction V_c cannot couple them.

In the derivation of Eqs. (2) through (9), Orbach assumes that the thermal distortions of the crystalline electric field are proportional to the local thermal strain and expands the crystal-field interaction in powers of the average strain ϵ.

$$\mathcal{H}_{cf}=\mathcal{H}_c+\epsilon V_c+\epsilon_1\epsilon_2 V_c+\cdots. \quad (10)$$

In this expansion $\mathcal{H}_c$ is the usual static crystal field[3,4,17]

$$\mathcal{H}_c=\sum_n\sum_{m=-n}^{n}B_n^m\langle r^n\rangle Y_n^m(\theta,\varphi)$$

$$=\sum_n\sum_{m=0}^{n}A_n^m G_n^m(x,y,z)$$

$$=\sum_n\sum_{m=0}^{n}A_n^m\langle r^n\rangle\chi_n O_n^m, \quad (11)$$

where $Y_n^m(\theta,\varphi)$ and $G_n^m(x,y,z)$ are normalized and unnormalized spherical harmonics, respectively, χ_n is an operator equivalent factor which depends upon the electronic configuration L, S, J, and the nature of the operator O_n^m (i.e., whether it consists of $J_\pm$, J_z or $L_\pm$, L_z), and O_n^m is an operator proportional to the matrix elements of $Y_n^m+Y_n^{-m}$. For a crystal such as $LaCl_3$ possessing C_{3h} symmetry, the (n,m) terms entering the sum in Eq. (11) are (2,0), (4,0), (6,0), and $(6,\pm 6)$.

The remaining terms in Eq. (10) constitute the orbit-lattice interaction $\mathcal{H}_c'$, and involve products of the two operators ϵ and V_c. The former is an ill-defined average of all thermal strain magnitudes, fluctuating randomly in time, and it enters the calculations as a phonon creation or destruction operator. We refer to V_c as the dynamic crystal field operator which is expressed by analogy with the static case as an expansion in spherical harmonics having the form

$$V_c=\sum_n\sum_{m=-n}^{n}b_n^m\langle r^n\rangle Y_n^m(\theta,\varphi). \quad (12)$$

In the expansion of the static crystal field, the axes can generally be chosen so that only the symmetric or cosine combination of the spherical harmonics, occur, i.e., $Y_n^m+Y_n^{-m}$ with the corresponding operator O_n^m. To describe the dynamic crystal-field expansion, one requires all even spherical harmonics which transform according to the irreducible representations of the normal modes of vibration of the complex composed of the paramagnetic ion and its immediate neighbors. For $LaCl_3$ the results are identical to those of the rare-earth

[17] M. T. Hutchings, *Solid State Physics* (Academic Press, New York, 1964), Vol. 16, p. 227.

ethyl sulfates,[2] where all m values consistent with $n=2$, 4, and 6 must be included. Furthermore, it is not generally possible to eliminate the antisymmetric or sine combination of the spherical harmonics so that terms such as $(Y_n^m-Y_n^{-m})/i$ are required. It is therefore convenient to define a set of Hermitian operators Θ_n^m such that $\Theta_n^{|m|}$ gives matrix elements proportional to $Y_n^m+Y_n^{-m}$ while $\Theta_n^{-|m|}$ yields results proportional to $(Y_n^m-Y_n^{-m})/i$. If the usual O_n^m operators, which occur in the literature, are made identical to $\Theta_n^{|m|}$ through the relation $\Theta_n^{|m|}=O_n^m=o_n^m+o_n^{-m}$ using the notation of Scott and Jeffries, then $\Theta_n^{-|m|}=(o_n^m-o_n^{-m})/i$.[18,19] Matrix elements of the Θ_n^m may be evaluated using the various tables[20] existing in the literature for the symmetric operators O_n^m, by noting the following relationships:

$$\langle J_z'|\Theta_n^{|m|}|J_z\rangle=\langle J_z'|O_n^m|J_z\rangle, \tag{13}$$

while

$$\langle J_z'|\Theta_n^{-|m|}|J_z\rangle=\pm i\langle J_z'|O_n^m|J_z\rangle, \tag{14}$$

where the + or − sign is chosen according to whether J_z is greater or less than J_z', respectively.

The operator equivalent formulation of Eq. (12) is then

$$V_c=\sum_{n=2,4,6}\sum_{m=-n}^{n}a_n^m\langle r^n\rangle\chi_n\Theta_n^m=\sum_{n,m}V_n^m, \tag{15}$$

where the $a_n^m\langle r^n\rangle$ are the dynamic crystal-field parameeters. Following Scott and Jeffries these parameters are approximated by the relation

$$|a_n^m\langle r^n\rangle|=g_n^{|m|}|A_n^0\langle r^n\rangle|, \tag{16}$$

where $g_n^{|m|}$ is a ratio of normalization constants and is tabulated for $|m|\leq n=2$, 4, and 6 in Ref. 7. It is through Eq. (16) that the optically determined static crystal-field parameters enter. Throughout all our calculations we have set $g_6^{|6|}$ equal to the experimental ratio of $A_6^6\langle r^6\rangle/A_6^0\langle r^6\rangle$ rather than the tabulated $g_6^{|6|}$ obtained from normalization constants.

The theoretical predictions for the direct, Orbach, and Raman coefficients all require the evaluation of matrix elements of the form $\langle J,J_z'|V_c|J,J_z\rangle=\langle J,J_z'|\sum_{n,m}V_n^m|J,J_z\rangle$. Since one has no knowledge concerning the phase coherence between the various V_n^m terms occurring in V_c, many authors feel the best approximation is obtained by assuming complete incoherence between the terms in the dynamic crystal field summation and therefore we set

$$|\langle i|V_c|j\rangle|^2=\sum_{n,m}|\langle i|V_n^m|j\rangle|^2. \tag{17}$$

To be explicit, we have evaluated the following expressions for the direct, Orbach, and Raman coefficients:

$$A=\frac{3k\delta^2}{\pi\rho v^5\hbar^4}\sum_{n,m}|\langle 1|V_n^m|2\rangle|^2, \tag{18}$$

$$B_i=\frac{3}{2\pi\rho v^5\hbar}\left(\frac{\Delta_i}{\hbar}\right)^3\frac{2\sum_{n,m}|\langle 1|V_n^m|i\rangle|^2\sum_{n,m}|\langle i|V_n^m|2\rangle|^2}{\sum_{n,m}|\langle 1|V_n^m|i\rangle|^2+\sum_{n,m}|\langle i|V_n^m|2\rangle|^2}, \tag{19}$$

$$C'=\frac{9!\hbar^2}{\pi^3\rho^2v^{10}}\left(\frac{k}{\hbar}\right)^9\sum_{i>2}\frac{\sum_{n,m}|\langle 1|V_n^m|i\rangle|^2\sum_{n,m}|\langle i|V_n^m|2\rangle|^2}{2\Delta_i^4}, \tag{20}$$

and

$$C+C''=\frac{9\times 6!}{4\pi^3\rho^2v^{10}}\left(\frac{k}{\hbar}\right)^7\left\{\sum_{n,m}|\langle 1|V_n^m|2\rangle|^2+\sum_{i>2}\frac{\sum_{n,m}|\langle 1|V_n^m|i\rangle|^2\sum_{n,m}|\langle i|V_n^m|2\rangle|^2}{\Delta_i^2}\right\}. \tag{21}$$

During previous consideration of the Raman process, it was noted that the matrix element $\langle 1|V_c|2\rangle$ vanishes when $|1\rangle$ and $|2\rangle$ are Kramers' conjugate states. A result of A equal to zero for Kramers' ions is avoided by applying the Zeeman interaction of Eq. (1) as a perturbation which mixes the states $|1\rangle$ and $|2\rangle$ with the excited crystal field states $|i\rangle$, breaking the time conjugate nature of the ground doublet. Thus $|1\rangle$ and $|2\rangle$ in Eqs. (3) and (18) must be replaced by $|1'\rangle$ and $|2'\rangle$, where

$$|1'\rangle=|1\rangle-\sum_{i>2}|i\rangle(\langle i|\mathcal{H}_z|1\rangle/\Delta_i) \tag{22}$$

and

$$|2'\rangle=|2\rangle-\sum_{i>2}|i\rangle(\langle i|\mathcal{H}_z|2\rangle/\Delta_i). \tag{23}$$

Using the fact that $\langle 1|V_c|2\rangle=0$ for Kramers' ions, the

[18] J. M. Baker and N. C. Ford, Phys. Rev. **136**, A1692 (1964).

[19] Our statement of the dynamic crystal field using the operators Θ_n^m is completely equivalent to the approach used by Baker and Ford (Ref. 18) if their V_n^m are multiplied by 2 and $2/i$ for m greater and less than zero, respectively.

[20] A complete set of the matrix elements of $O_n^{|m|}(n=2,4,6)$ for integer and half-integer values of angular momentum through $J=8$ tabulated in decimal form by computer and reproduced photographically is available from the authors.

direct process matrix element has the form

$$|\langle 1'|V_c|2'\rangle|^2=\left|\sum_{i>2}\frac{\langle 1|V_c|i\rangle\langle i|\mathcal{H}_z|2\rangle}{\Delta_i}+\sum_{i>2}\frac{\langle 1|\mathcal{H}_z|i\rangle\langle i|V_c|2\rangle}{\Delta_i}\right|^2, \quad (24)$$

where we have carried the sum over all excited states of the ground J multiplet. Similar Zeeman admixtures for the other processes are usually neglected because their contribution is negligible. Due to the second-order nature of the Kramers' direct process, non-Kramers ions should possess a larger direct process coefficient, A.

Since the Zeeman interaction is generally anisotropic, the relaxation calculations which have been described should show an angular dependence. It is enlightening to divide this effect into two parts. The first is an interaction solely within each magnetic doublet in which the proper wave functions $|i\rangle$ and $|j\rangle$ to be used in Eqs. (18)–(21) are those orthogonal linear combinations which diagonalize the spin Hamiltonian pertinent to the doublet in question. For the ground doublet in particular, this is expressed as

$$|1\rangle=\alpha(\theta)|a\rangle-\eta(\theta)|b\rangle,$$
$$|2\rangle=\eta(\theta)|a\rangle+\alpha(\theta)|b\rangle, \quad (25)$$

where $\eta(\theta)$ is zero if $g_\perp$ is zero. Thus this contribution to the angular dependence is zero for each doublet of a non-Kramers' ion.

The second contribution to the angular variation depends upon the admixture of excited-state wave functions ($|n\rangle$, for $n>2$) into the ground doublet via the Zeeman Hamiltonian of Eq. (1). This has already been considered in removing the time-reversal symmetry of Kramers pairs through Eq. (24), but the admixture aspect applies equally well to non-Kramers' ions. These admixtures will depend upon θ and will be the sole source of theoretical relaxation anisotropy which we consider for non-Kramers' ions.

For each ion except cerium and samarium the relaxation coefficients given by Eqs. (18)–(21) have been evaluated for various angles θ using an IBM 7094 computer. Ce^{3+} and Sm^{3+} each possess a $J=5/2$ ground level within which χ_6 of Eq. (15) is zero. For these ions it is necessary to consider admixtures from the excited $J=7/2$ manifold. This complication is beyond our present FORTRAN program so these ions were treated by hand calculation.

Since matrix elements of the form $\sum_{i>2}\langle 1|V_n^m|i\rangle\times\langle i|V_n^m|1\rangle$, together with a similar term involving state $|2\rangle$, occur in the evaluation of B and C', it is natural to expect the Orbach and Raman relaxation rates of Kramers' ions to show some angular variation since the wave functions $|1\rangle$ and $|2\rangle$ vary with θ in a manner prescribed by Eq. (25). The variation of the excited states $|i\rangle$ ($i>2$) with angle should not produce any anisotropy because of closure properties. For those Kramers ions treated by our computer program, i.e., Nd and Er, the calculations predict an anisotropy in B of 50% for Nd and 6.5% for Er. Similar calculations for the Raman process predict a 10% anisotropy for both ions. Since Nd does not exhibit a detectable Orbach relaxation mechanism experimentally (see Sec. IIIC) and because our experimental error is roughly 10%, no angular variations in the Orbach or Raman process were observed for these or any other ions which we studied.

Up to this point is has been assumed that the transitions involved in the process of spin-lattice relaxation have not disturbed the thermal equilibrium of the phonon system. If, however, a spin system relaxing via the direct process creates phonons of energy $\delta=h\nu$ faster than these phonons can thermalize by giving up their energy to the helium bath or the remainder of the phonon system, the spin system will find itself interacting with phonons at some effective temperature which is greater than the bath temperature and the measured relaxation rate will be slowed. This process has become known as the "phonon bottleneck."[21–24]

In the case of a bottlenecked direct process, the Orbach calculation must be replaced by a treatment which takes into account the return of the coupled spin-phonon system to thermal equilibrium. The result of such a calculation is a predicted relaxation rate $1/\tau_1$ given by[7]

$$1/\tau_1\approx DT^2, \quad (26)$$

with

$$D=(6k^2/\pi^2\hbar^3)(\Delta\delta/cv^3)(1/T_{\rm ph}), \quad (27)$$

where $\Delta\delta=h\Delta\nu\approx g\beta\Delta H$ is the bandwidth of the phonons interacting with the spin system, c is the number of paramagnetic spins per unit volume, v is the velocity of the phonons of energy $\delta=h\nu$, and $1/T_{\rm ph}$ is the assumed rate at which the phonons return to thermal equilibrium in the absence of interactions with spins. The direct process is expected to display a bottleneck when $\tau_1>T_{1d}$ or $DT^2\ll AT$.

To summarize this section, we expect the observed spin-lattice relaxation rate of a given ion to be the sum of the rates of the three competing direct, Orbach, and Raman processes such that

$$T_1^{-1}=T_{1d}^{-1}+T_{10}^{-1}+T_{1R}^{-1}. \quad (28)$$

Each relaxation mechanism will display a characteristic temperature dependence and the anisotropic Zeeman interaction should produce an angular dependence. Finally, the fact that the phonon system has a finite specific heat admits the possibility of a phonon bottle-

[21] J. A. Giordmaine and F. R. Nash, Phys. Rev. **138**, A1510 (1965). This recent paper includes a list of references to both experimental and theoretical work on this phenomenon.
[22] I. M. Firth and D. Bijl, Phys. Letters **2**, 160 (1962).
[23] A. R. Miedema and K. W. Mess, Physica **30**, 1849 (1964).
[24] W. J. Brya and P. E. Wagner, Phys. Rev. Letters **14**, 431 (1965).

neck where the observed spin-bath relaxation rate is slower than the true spin-phonon relaxation.

III. EXPERIMENTAL

The host lattice of $LaCl_3$ crystallizes with a structure whose space symmetry is $C6_3/m(C_{6h}^2)$[25]; the point symmetry at the site of the La^{3+} ion is C_{3h}. Nine nearly equidistant Cl^- ions surround La^{3+}; three at a distance of 2.97 Å form an equilateral triangle coplanar with the La^{3+} ion while the remaining six are located 2.99 Å away at the vertices of two equilateral similar triangles in planes above and below the La^{3+} site. The unit cell contains two magnetically equivalent lanthanum ions and the density of the crystal is 3.84 g/cm³.[26] The sound velocity of 10 Mc/sec longitudinal waves in $LaCl_3$ was measured at room temperature using a pulse-echo technique.[27] The direction of propagation was ostensibly along the c axis and severe acoustic attenuation hindered accurate measurements. The best estimate is 2×10^5 cm/sec.

Hutchison and Wong[14] have reported the electron spin resonance of rare-earth ions in $LaCl_3$. Their data for Kramers' ions were fit to a spin Hamiltonian of the form

$$\mathcal{H}_s=g_{\parallel}\beta H_zS_z+g_{\perp}\beta(H_xS_x+H_yS_y)+hcAI_zS_z +hcB(I_xS_x+I_yS_y)+hcP[I_z^2-\tfrac{1}{3}I(I+1)], \quad (29)$$

where $S=1/2$ and I is the nuclear spin of the rare-earth isotope. For non-Kramers ions $g_{\perp}$ and B are identically zero and a term $hc(\Delta_xS_x+\Delta_yS_y)$ is required in Eq. (29) to account for the existence of a resonance and to describe a zero-field splitting of the order of $\Delta=(\Delta_x^2+\Delta_y^2)^{1/2}$ cm^{-1}. No resonance was expected or observed for Dy, Yb, or Tm.[14] Eu^{3+} ($J=0$) and radioactive Pm were not studied in the trichloride. Experiments to measure the relaxation rate of Pm in $LaCl_3$ are being initiated in this laboratory. To date Pm^{3+} has been reported only in the ethyl sulfate[28] where radiation damage rapidly broadens the resonances until they become undetectable.

Single crystals of $LaCl_3$ were prepared using a composite of standard techniques.[14,29] The critical step of desiccating the hydrated salt was performed without the use of any drying gas, using instead a diffusion pump and slowly elevated temperatures. The dehydration, sublimation, and crystal growth were all carried out in an uninterrupted vacuum. The final samples were cylindrical, 4 mm in diameter, and 5–8 mm long. All reported concentration values refer to the starting material $LaCl_3\cdot7H_2O$. No attempt has been made to measure the actual doping of the final sample, which could be different due to ionic selectivity during sublimation and crystallization. $LaCl_3\cdot7H_2O$ was prepared by reacting La_2O_3 (rare-earth purity $\geq$99.997%) with reagent-grade HCl and distilled water. Doping solutions with a rare-earth purity of 99.9% were prepared similarly.

The hygroscopic samples were stored in mineral oil between experiments. During measurements they were given a protective coating of Apiezon N grease and then usually encased in an open-ended Teflon cylinder which was mounted in the microwave cavity. All measurements were made with liquid helium in the cavity and the observed relaxation rates showed no effects due to temperature cycling of the samples or to mounting details. The relaxation times were measured using pulse-saturation techniques similar to those described by Scott.[7] The resonance signal was detected using a superheterodyne X-band spectrometer nearly identical to that employed by Raubenheimer.[13] One significant difference was the use of a calibrated exponential voltage generator[30] to provide a horizontal oscilloscope sweep in the range from 1 sec to 1 μsec. By adjusting the time constant of the generator until the signal recovery appeared as a straight line on the oscilloscope, we were able to measure relaxation times directly and eliminate the need for photographs except for very long relaxation times. Some ions did not exhibit a single exponential recovery (see Sec. IV) and in these instances the quoted relaxation times refer to the rates measured at the extreme end of the recovery. Provided that a sufficient degree of signal saturation occurred to permit measurements in the tail of the recovery, the results were independent of the pulse length which varied from ion to ion in the range between 100 μsec and 1 sec. All data were obtained with monitor power levels at least 5 dB below the onset of any detectable saturation effects.

Data were collected as a function of the temperature and orientation of the magnetic field. An individual measurement is considered accurate to about ±10%, and a single data point on the figures of Sec. IV represents the average of 3–15 measurements. The data were fitted in a weighted least-squares sense to the temperature dependence expected from the theoretical considerations of Sec. II, and the best fitting values of A, B, C', and $C+C''$, or D are presented in Sec. IV.

IV. RESULTS

A. Cerium, $4f^1$

The paramagnetic resonance spectrum of naturally abundant Ce^{3+} in $LaCl_3$ consists of a single line described by $g_{\parallel}=4.0366\pm0.0015$ and $g_{\perp}=0.17\pm0.08$.[14]

[25] W. H. Zachariasen, J. Chem. Phys. **16**, 254 (1948).
[26] *Handbook of Chemistry and Physics*, edited by C. D. Hodgman, (Chemical Rubber Publishing Company, Cleveland, 1955), 37th ed., p. 531.
[27] We are indebted to K. Swartz for this measurement.
[28] H. J. Stapleton, C. D. Jeffries, and D. A. Shirley, Phys. Rev. **124**, 1455 (1961).
[29] D. M. Gruen, J. C. Conway, and R. E. McLaughlin, J. Chem. Phys. **25**, 1102 (1956). In addition we received helpful information in the form of private communications with C. A. Hutchinson, Jr., B. W. Mangum, and M. Abraham.
[30] N. Ford and C. D. Jeffries (private communication).

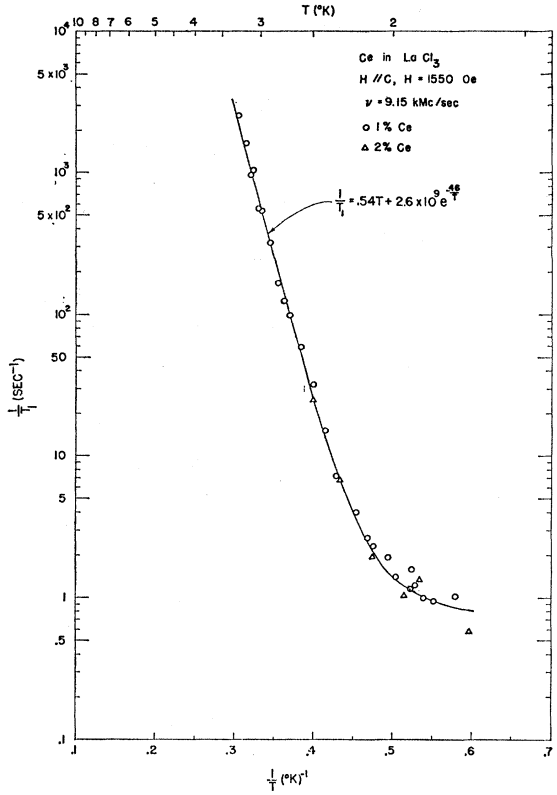

FIG. 2. Relaxation data for 1 and 2% Ce^{3+} in $LaCl_3$ at 9.15 kMc/sec with the magnetic field parallel to the crystal axis. The linear portion of the plot at the higher temperatures corresponds to a dominant Orbach process. At temperatures below 2°K the direct process is most important.

Cerium is the only ion studied in this paper for which optical data are not available. As an alternative we have estimated the energy levels and wave functions by: taking 640 cm^{-1} as the spin-orbit coupling constant[31,32]; setting $A_6{}^6\langle r^6\rangle/A_6{}^0\langle r^6\rangle=-10$ (a value consistent with the other rare earths in $LaCl_3$); estimating $A_4{}^0\langle r^4\rangle$ and $A_6{}^0\langle r^6\rangle$ by extrapolation from heavier rare earths[33]; and determining the value of $A_2{}^0\langle r^2\rangle$ necessary to set the first excited crystal-field state approximately 32 cm^{-1} above the ground doublet (a value consistent with our relaxation data for the Orbach process).[34,35] The resulting crystal-field parameters are listed in Table I.

TABLE I. Estimated crystal-field splittings and wave functions for Ce^{3+} ($4f^1$, $^2F_{5/2}$ and $^2F_{7/2}$) in $LaCl_3$ using the crystal-field parameters $A_2{}^0\langle r^2\rangle=50$ cm^{-1}, $A_4{}^0\langle r^4\rangle=-40$ cm^{-1}, $A_6{}^0\langle r^6\rangle=-45$ cm^{-1}, and $A_6{}^6\langle r^6\rangle=450$ cm^{-1} and a spin-orbit coupling constant $\zeta=640$ cm^{-1}. The kets are written as $|L_z,S_z\rangle$ with $L=3$ and $S=\frac{1}{2}$.

n	E_n (cm^{-1})	Wave functions $\|n\rangle$ for $\theta=0°$
13, 14	2400	$0.515\|\mp2,\pm\rangle+0.857\|\mp1,\mp\rangle$
11, 12	2340	$0.759\|\mp2,\mp\rangle+0.340\|\mp3,\pm\rangle-0.556\|\pm3,\pm\rangle$
9, 10	2250	$0.710\|\mp1,\pm\rangle+0.705\|0,\mp\rangle$
7, 8	2210	$0.828\|\pm3,\pm\rangle+0.540\|\mp2,\mp\rangle+0.150\|\mp3,\pm\rangle$
5, 6	105	$0.857\|\mp2,\pm\rangle-0.515\|\mp1,\mp\rangle$
3, 4	33	$0.710\|0,\mp\rangle-0.705\|\mp1,\pm\rangle$
1, 2	0	$0.928\|\mp3,\pm\rangle-0.365\|\mp2,\mp\rangle+0.070\|\pm3,\pm\rangle$

The ground level of the $4f^1$ configuration of Ce^{3+} is $^2F_{5/2}$ but it is necessary to include admixtures of the excited level $^2F_{7/2}$ in order to account for the nonzero value of $g_\perp$ for the lowest crystal-field doublet. We have accomplished this by simultaneously diagonalizing the spin-orbit and crystal field interactions. The resulting energy levels and wave functions are listed in Table I using the representation $|L=3, S=1/2, L_z, S_z\rangle$ since it simplifies the calculations between two J levels. The resulting theoretical g values for the ground doublet are $g_\parallel=4.28$ and $g_\perp=0.134$.

Our measured relaxation rates for crystals containing 1% and 2% Ce^{3+} are shown in Fig. 2. The data indicate no concentration dependence in this range and show a very rapid temperature dependence which can be fitted to the expression

$$1/T_1=0.54T+2.6\times10^9\exp(-46/T)\ \text{sec}^{-1} \quad (30)$$

when the magnetic field is parallel to the crystal c axis. These values for A, B, and Δ_3 are obtained from a weighted least-squares fit of the data to Eq. (28) and have probable errors of ±0.02 $sec^{-1}°K^{-1}$, $\pm0.5\times10^9$ sec^{-1}, and ±3°K, respectively. Single exponential recoveries were observed over the entire temperature range which was limited at the high end by our inability to sufficiently saturate the resonance line.

In Fig. 3, measurements of the angular dependence of the total relaxation rate of 1% Ce^{3+} are plotted at four temperatures as a function of the magnetic field orientation θ. These plots indicate that the anisotropy is strongest at those temperatures where the relaxation is predominantly via the direct mechanism. Assuming that the Orbach relaxation rate is isotropic, one can compute the experimental anisotropy in the direct process coefficient, $A(\theta)$, from the data of Fig. 3. The resultant points are plotted in Fig. 4 where errors represent the effects of averaging data at several temperatures. The smallness of these errors indicates the validity of assuming an isotropic Orbach process.

Using the energy levels and wave functions for $\theta=0°$ which are listed in Table I, we calculate a B value of 2.70×10^{11} sec^{-1}. The angular dependence of the direct process coefficient A is somewhat involved. An inspection of the wave functions listed in Table I indicates

[31] R. J. Lang, Can. J. Res. **14**, 127 (1936).
[32] A. J. Freeman and R. E. Watson, Phys. Rev. **127**, 2058 (1962).
[33] G. Burns, J. Chem. Phys. **42**, 377 (1965). It has been pointed out to us by R. Orbach that our extrapolated crystal field parameters for Ce^{3+} may be in error owing to the absence of correlation effects for a $4f^1$ configuration.
[34] B. Schneider, Z. Physik **177**, 179 (1964). These magnetic susceptibility measurements on 100% $CeCl_3$ indicate $\Delta_3=68\pm5$°K (47 cm^{-1}).
[35] Hutchinson and Wong (Ref. 14) calculated an energy splitting of $\Delta_3=45.7$ cm^{-1} and $\Delta_5=112.7$ cm^{-1} using crystal field parameters for Pr^{3+}.

that for $\theta=0°$ all Zeeman admixtures into states $|a\rangle$ and $|b\rangle$ originate from states $|7\rangle$, $|8\rangle$, $|11\rangle$, and $|12\rangle$ of the excited $J=7/2$ manifold. The result is $A(0°)=A_{7/2}=0.703\times10^{-2}$ sec^{-1} °K^{-1}, which is about 1/80 of the experimental value. For $\theta\neq0°$ the ground doublet is mixed with the much closer states $|5\rangle$ and $|6\rangle$ of the $J=5/2$ manifold. Because of the difficulty involved in a hand calculation of the angular dependence of the admixtures from the $J=7/2$ manifold and since the contributions from the ground $J=5/2$ manifold soon exceed the former as **H** is moved away from the c axis, we have considered $A_{7/2}$ to be a constant independent of θ and have written the total direct process coefficient for Ce in the form $A(\theta)=A_{7/2}+A_{5/2}(\theta)$. In order to

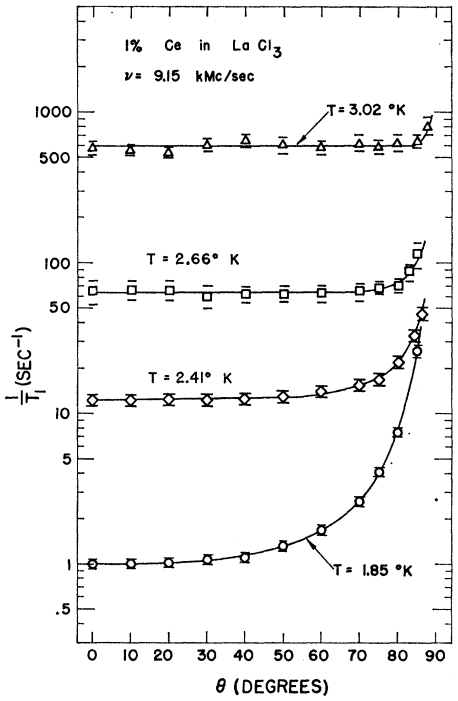

FIG. 3. Angular dependence of the observed total relaxation rate of 1% Ce^{3+} in $LaCl_3$ at 9.15 kMc/sec at four different temperatures.

emphasize the proportional agreement between theory and experiment, Fig. 4 contains a "normalized" theoretical curve of the form $C_1+C_2A(\theta)$, where C_1 equals the experimental value of A at $\theta=0°$ and C_2 is 1/13.5. It is interesting to note that the theoretical expression for $A(\theta)$ maximizes somewhere between 88.6° and 89.0°.

The lack of numerical agreement for this case of Ce^{3+} may be due to our lack of good wave functions and energy levels, but the correct angular behavior indicates the general validity of this approach pending improved static crystal field parameters from optical data.

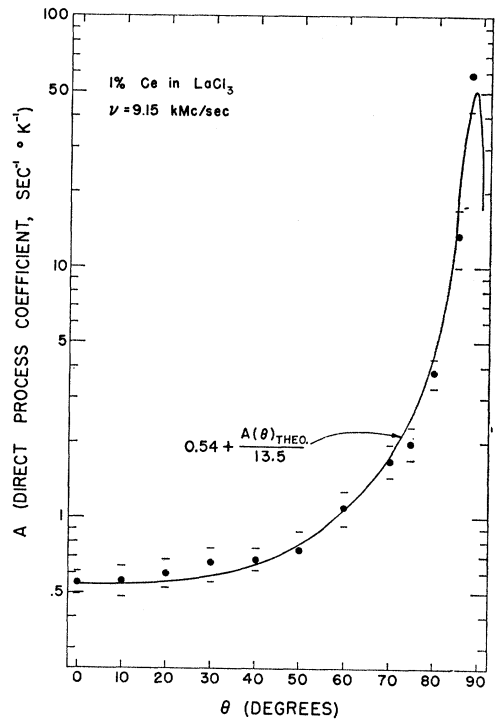

FIG. 4. Observed angular dependence of the direct process coupling coefficient $A(\theta)$ for 1% Ce^{3+} in $LaCl_3$ at 9.15 kMc/sec as deduced from the data of Figs. 2 and 3 by assuming that the Orbach mechanism is isotropic. The solid curve is a "normalized" theoretical result which is forced to fit the datum at $\theta=0°$ by the addition of additive and multiplicative constants to the theoretical expression.

B. Praseodymium, $4f^2$

Praseodymium trichloride has been the object of considerable optical study.[36] The ground level $^3H_4$ splits under the action of a crystal field of C_{3h} symmetry into three doublets and three singlets. Margolis[37] has presented the most complete analysis of the optical spectra of Pr^{3+} in $PrCl_3$, deriving the crystal-field parameters[38]

TABLE II. Experimental crystal field splittings[a] and calculated wave functions for the ground level of Pr^{3+} ($4f^2$, $^3H_4$) in $LaCl_3$. The wave functions are computed using the crystal field parameters listed in the text and are written in terms of $|J_z\rangle$ with $J=4$.

n	E_n (cm^{-1})	Wave functions $\|n\rangle$ for $\theta=0°$
9	(210.0)[b]	$\|0\rangle$
8	137.0	$0.707\|3\rangle+0.707\|-3\rangle$
6, 7	130.2	$\|\pm1\rangle$
4, 5	96.4	$0.883\|\pm4\rangle+0.469\|\mp2\rangle$
3	33.1	$0.707\|3\rangle-0.707\|-3\rangle$
1, 2	0.0	$0.883\|\pm2\rangle-0.469\|\mp4\rangle$

[a] See Ref. 36.
[b] Calculated value.

[36] R. Sarup and M. H. Crozier, J. Chem. Phys. **42**, 371 (1965) and Refs. 1–7 of this paper.
[37] J. S. Margolis, J. Chem. Phys. **35**, 1367 (1961).
[38] These values are credited to Margolis (private communication) by M. T. Hutchings and D. K. Ray, Proc. Phys. Soc. (London) **81**, 663 (1963).

$A_2^0\langle r^2\rangle = 47.26$ cm^{-1}, $A_4^0\langle r^4\rangle = -40.58$ cm^{-1}, $A_6^0\langle r^6\rangle = -39.62$ cm^{-1}, and $A_6^6\langle r^6\rangle = 405.4$ cm^{-1}. Table II lists the experimentally observed energy levels and our calculated wave functions for dilute Pr^{3+} in $LaCl_3$.

The spin-Hamiltonian parameters reported by Hutchison and Wong[14] are $g_{\parallel} = 1.035 \pm 0.005$, $A = (5.02 \pm 0.03) \times 10^{-2}$ cm^{-1}, $I = 5/2$, and $\Delta \approx 0.02$ cm^{-1}. Praseodymium exhibits the usual asymmetric line shape which distinguishes most non-Kramers ions.[39] Our 1% and 0.3% samples both had linewidths of 29 Oe (full width at half-maximum absorption) at $\theta = 0°$. The calculated $g_{\parallel}$ of 1.09 obtained from state $|1\rangle$ of Table II agrees quite well with the experimental value.

All of the presented relaxation data were obtained from measurements made on the lowest field hyperfine line. Brief checks for the dependence of the relaxation rate on the nuclear spin state were made at various temperatures. Above 2.3°K no I_z dependence was observed within the experimental accuracy of $\pm 10\%$. At 2°K the observed relaxation rates became slower as one progressed among the hfs in order of increasing field. The highest field line relaxed at about 60% the rate of the lowest field line. All recovery signals were nonexponential and we were unable to determine if the whole resonance line was being saturated.

The relaxation data for 1% Pr^{3+} at $\theta = 0°$ could be fit by the expression

$$1/T_1 = 272T^2 + 2.06 \times 10^9 \exp(-47.9/T) \text{ sec}^{-1}, \quad (31)$$

as shown in Fig. 5. We have interpreted this as representing a normal Orbach process and a bottlenecked direct process. At the lowest temperatures, where the Orbach process is negligible, the fit to a T^2 dependence is quite definite. The uncertainties in these coefficients are estimated to be ± 5 sec^{-1} °K^{-2} for D and $\pm 0.14 \times 10^9$ sec^{-1} for B. A least-squares fit indicated that Δ_3 was 46.2 ± 3°K which is in good agreement with the optical value of 47.9°K. The theoretical bottleneck coefficient, D, is expected to be inversely proportional to the spin concentration. Data for a sample containing 0.3% Pr^{3+} are also shown in Fig. 5. The weaker signals obtained from this crystal prevented our taking measurements at a sufficiently high temperature to establish the strength of the Orbach process. Alternatively we assumed it to be unchanged from the 1% sample and then a bottleneck factor of D equal to 1106 ± 30 sec^{-1} °K^{-2} was obtained as a best fit of the data. The experimental ratio of these bottleneck coefficients is 4.07 as opposed to an estimated concentration ratio of 10/3. Since the paramagnetic resonance (PMR) linewidths did not change, this discrepancy may be due to our imprecise knowledge of the actual sample dopings. It is important to emphasize again that these results were repeatable even after temperature cycling.

The bottleneck coefficient is also expected to be directly proportional to the bandwidth $\Delta\nu$ of the phonons which can interact with the spins via a direct process. Assuming that $\Delta\nu$ is related to the spin-resonance linewidth, a plot of D versus $g\Delta H$ should be linear according to the theory. For this material $g\Delta H$ varies with magnetic field orientation and the data of Fig. 6 were obtained by measuring the bottlenecked relaxation rate and the PMR linewidth at various angles θ. In this presentation ΔH is the full width at half-maximum absorption and g is simply $g_{\parallel} \cos\theta$ since $g_{\perp}$ is zero. Unfortunately, the shape of the PMR line changes as well as the width, as evidenced by the fact that the ratio of ΔH to the peak-to-peak derivative width also changes with θ. This complication may explain the slightly nonlinear behavior of the experimental points in Fig. 6; however, more fundamental questions concerning the proper relationship of $\Delta\nu$ to ΔH are undoubtedly pertinent.[21]

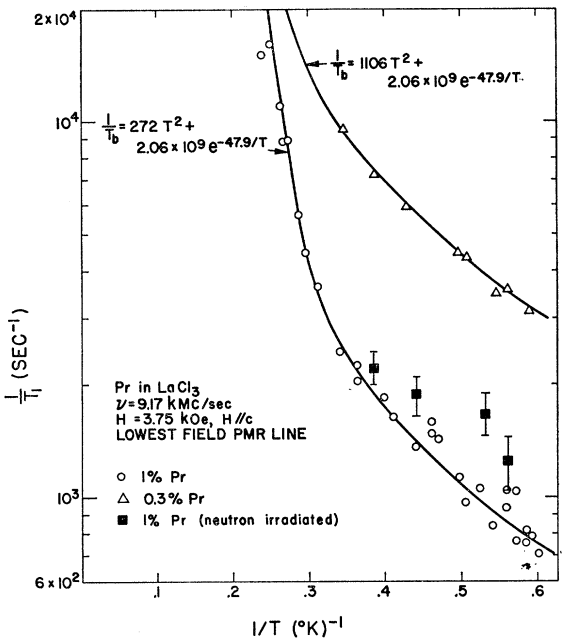

FIG. 5. Relaxation data for 0.3 and 1.0% Pr^{3+} in $LaCl_3$ at 9.17 kMc/sec with the magnetic field parallel to the crystal axis. The concentration effects and the T^2 temperature effects indicate a direct process which is phonon-limited. The phonon bottleneck of the 1% sample is apparently reduced by neutron bombardment.

Our theoretical calculations for the normal (unbottlenecked) processes predict that $A = 1.79 \times 10^5$ sec^{-1} °K^{-1}, $B = 2.81 \times 10^{10}$ sec^{-1}, and $(C + C'') = 0.0733$ sec^{-1} °K^{-7}. This value of B is about ten times greater than the experiments indicate, while the C coefficient is within 20% of the experimental value if a Raman term is included in the fit. It has been omitted from Eq. (31) since its inclusion diminishes the standard deviation of the fit by only 1%. The fact that the direct process appears to be bottlenecked is consistent with the condition that $DT^2 \ll AT$ using the experimental D and theoretical A values.

Using Eq. (27) with $\Delta H = 30$ Oe for a 1% doping, we

[39] J. M. Baker and B. Bleaney, Proc. Roy. Soc. (London) A245, 156 (1958).

find that T_{ph} is about 80 nsec if D is equal to 272 sec^{-1} $°K^{-2}$. This very short phonon equilibration time corresponds to a path length of the order of 160 μ. This should be contrasted to the results of other bottlenecked salts[7,8] where the equilibration length is usually limited by the sample size. Measurements on our crystal after cleavage along the c axis yielded unaltered relaxation times. Adopting a purely experimental approach in an effort to alter this length, we subjected the 1% sample to 100-keV x rays for 24 h and observed no change in the relaxation rate. Next the sample was bombarded with fast neutrons in a flux of the order of 10^{13} n/cm^2 sec for 1 h. Upon subsequent examination about two weeks later, the relaxation rate was larger by a factor of about 1.5. Since no detectable change occurred in the PMR linewidth, this corresponds to a phonon equilibration time of about 53 nsec. This result is very surprising since one would not expect any energy degradation for a phonon-defect collision under these circumstances.

C. Neodymium, $4f^3$

The paramagnetic resonance spectrum of naturally abundant Nd consists of a strong central line due to the five even-even isotopes of Nd (79.5% abundant) flanked by two sets of weaker hyperfine lines originating from Nd^{143} (12.2% abundant) and Nd^{145} (8.3% abundant) both with a nuclear spin of 7/2. Our relaxation measurements were all made on the strong central line described by[14] a $g_{\parallel}$ of 3.996±0.001 and a $g_{\perp}$ of 1.763 ±0.001. This main resonance line displays a considerable amount of angularly dependent structure which apparently is due to Nd-Nd pair interactions.[40] These pair spectra may explain the fact that the signal recoveries were not exponential and appeared to be weakly concentration-dependent.[41] The absorption derivative exhibited a fairly isotropic peak-to-peak linewidth of about 6 Oe in the case of a 0.1% doping and 13 Oe for a 2% doping.

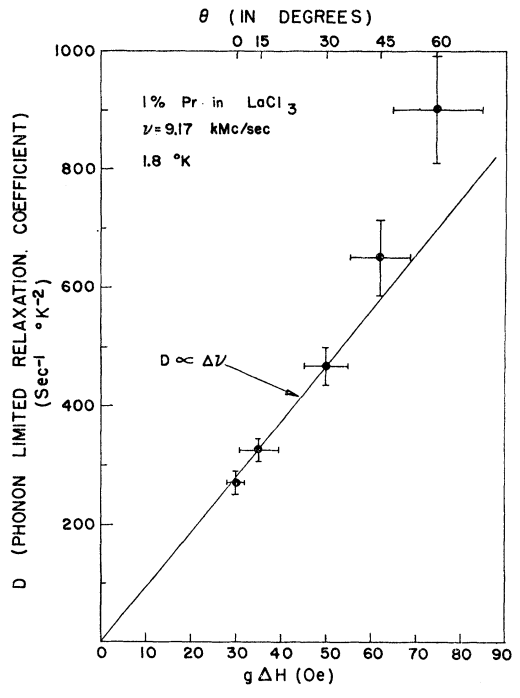

FIG. 6. The phonon bottleneck coefficient for 1% Pr^{3+} in $LaCl_3$ at 9.17 kMc/sec and 1.8°K plotted against a parameter $g\Delta H$ which is proportional to the frequency bandwidth of the paramagnetic resonance. Here ΔH is defined as the full width at half-maximum absorption. These data are collected by measuring the relaxation rate and the linewidth as a function of θ.

TABLE III. Experimental crystal-field splittings[a] and calculated wave functions for the ground level of Nd^{3+} ($4f^3$, $^4I_{9/2}$) in $LaCl_3$. The wave functions are computed using the crystal field parameters listed in the text and are written in terms of $|J_z\rangle$ with $J=\frac{9}{2}$.

n	E_n (cm^{-1})	Wave functions $\|n\rangle$ for $\theta=0°$
9, 10	249.4	$0.936\|\pm\frac{5}{2}\rangle-0.351\|\mp\frac{7}{2}\rangle$
7, 8	244.4	$0.558\|\pm\frac{9}{2}\rangle-0.830\|\mp\frac{3}{2}\rangle$
5, 6	123.2	$0.830\|\pm\frac{9}{2}\rangle+0.558\|\mp\frac{3}{2}\rangle$
3, 4	115.4	$\|\pm\frac{1}{2}\rangle$
1, 2	0.0	$0.351\|\pm\frac{5}{2}\rangle+0.936\|\mp\frac{7}{2}\rangle$

[a] See Ref. 42.

Eisenstein's[42] crystal-field parameters ($A_2^0\langle r^2\rangle=97.59$ cm^{-1}, $A_4^0\langle r^4\rangle=-38.67$ cm^{-1}, $A_6^0\langle r^6\rangle=-44.44$ cm^{-1}, and $A_6^6\langle r^6\rangle=443.00$ cm^{-1}) were used to obtain the wave functions of the ten Kramers doublets which arise from the crystal-field splitting of the $^4I_{9/2}$ ground level of Nd^{3+} in $LaCl_3$. The observed energy splittings and the calculated wave functions are listed in Table III. The fact that the first excited crystal-field states lie 166°K above the ground doublet makes an active Orbach mechanism very improbable. The calculated g values for the ground doublet are $g_{\parallel}=4.02$ and $g_{\perp}=1.91$.

Temperature measurements on the relaxation times of Nd^{3+} in $LaCl_3$ were complicated by angular effects displayed in Fig. 7 which shows two distinct maxima in the relaxation rates near $\theta=18°$ and 80°. The pronounced peak at 18° is probably due to cross relaxation between Nd^{3+} ions and an otherwise undetected Ce^{3+} impurity. The two resonances should cross at about this angle and the extreme temperature dependence of the cerium relaxation explains the reduction in the effect as the temperature is lowered. The cause of the smaller peak around 80° is not certain,[43] but the fact that only the 80° peak disappeared when the experi-

[40] K. L. Brower (private communication).

[41] The samples containing 1% Nd relaxed about 50% faster than the 0.1% doped crystals. Note that this concentration dependence is much weaker and opposite to the type expected for a phonon bottleneck.

[42] J. C. Eisenstein, J. Chem. Phys. **39**, 2134 (1963).

[43] A similar effect was observed by Scott and Jeffries (Ref. 7) for Nd in lanthanum ethyl sulfate where they identified the two peaks as due to cross relaxation with the two lowest doublets of cerium. However, in the ethyl sulfate the first excited Ce^{3+} state is only 3.94 cm^{-1} above the ground doublet while it is apparently at least 32 cm^{-1} removed in the trichloride. This makes such an explanation unlikely for our case in spite of the fact that the resonances would overlap at approximately 78°.

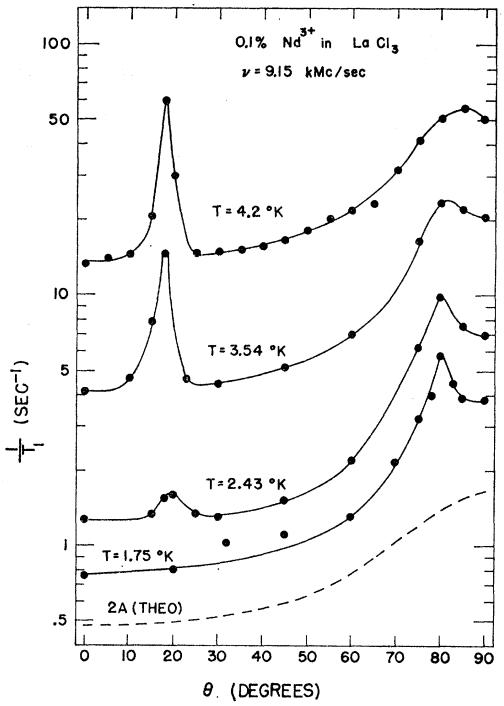

FIG. 7. Angular dependence of the observed total relaxation rate of 0.1% naturally abundant Nd^{3+} in $LaCl_3$ at four different temperatures. The theoretically expected anisotropy for the direct process rate at $T=2°K$ is indicated by the dashed curve.

ments were repeated with enriched isotopes of Nd (97.7% even-even) points to possible cross relaxation effects between Nd ions with and without nuclear spin. Neglecting the peak around 18°, the even-even Nd data approached $\theta=90°$ with an angular dependence similar to that shown by the theoretical curve drawn for $T=2°K$ in Fig. 7.

It was not possible to fit either the 1% or the 0.1% Nd data for $\theta=0°$ or 90° to an equation of the form $1/T_1=AT+C'T^9$. The most likely reason is that the mechanisms responsible for the temperature-dependent peaks at 18° and 80° are probably still important at $\theta=0°$ and 90°. Therefore we have attempted a fit at $\theta=45°$ and the resulting data are presented in Fig. 8 for a sample doped with 0.1% enriched Nd. The best fit to a direct and Kramers-Raman process is

$$1/T_1=0.581T+4.85\times10^{-5}T^9 \text{ sec}^{-1}, \qquad (32)$$

where the probable errors in A and C' are ±0.016 sec^{-1} $°K^{-1}$ and $\pm0.12\times10^{-5}$ sec^{-1} $°K^{-9}$, respectively. The theoretical estimates of A, B, and C' using the energies and wave functions listed in Table III and evaluated for $\theta=45°$ are: $A=0.295$ sec^{-1} $°K^{-1}$, $B=1.22\times10^{12}$ sec^{-1}, and $C'=3.75\times10^{-5}$ sec^{-1} $°K^{-9}$. Agreement with the experimental A and C' values is thus within a factor of 2 while the Orbach process is predicted as negligible when the exponential factor is included.

D. Samarium, $4f^5$

The two lowest levels of a free Sm^{3+} ion are $^6H_{5/2}$ and $^6H_{7/2}$ separated by about 1040 cm^{-1}. Analysis of optical data from the trichloride[44] indicates that the lowest lying crystal-field states are predominantly $|J=5/2, J_z=\pm1/2\rangle$ at 0 cm^{-1}, $|J=5/2, J_z=\pm3/2\rangle$ at 40.7 cm^{-1}, and $|J=5/2, J_z=\pm5/2\rangle$ at 66.1 cm^{-1}.[45] As in the case of Ce^{3+} ($^2F_{5/2}$), the existence of a ground level with a J value less than three necessitates more complicated calculations which are beyond the capabilities of our present FORTRAN computer program. It is necessary to include wave function admixtures from the $J=7/2$ manifold due to the static crystal field. Using the parameters[45] $A_2{}^0\langle r^2\rangle=80.85$ cm^{-1}, $A_4{}^0\langle r^4\rangle=-22.75$ cm^{-1}, $A_6{}^0\langle r^6\rangle=-44.39$ cm^{-1}, and $A_6{}^6\langle r^6\rangle=425.7$ cm^{-1} and first-order perturbation theory the augmented wave functions listed in Table IV are obtained.

Naturally abundant samarium is composed of 71.2% even-even isotopes, 15% Sm^{147} ($I=7/2$), and 13.8% Sm^{149} ($I=7/2$). The hfs of the odd isotopes is well resolved from the single line of the even-even isotopes. This main transition is characterized[14] by a $g_{\parallel}$ of 0.5841 ± 0.0003 and a $g_\perp$ of 0.6127 ± 0.0006. Using states $|1\rangle$ and $|2\rangle$ of Table IV we obtain $g_{\parallel}=0.546$ and $g_\perp=0.700$. Single crystals of $LaCl_3$ doped with trivalent samarium are very difficult to grow.[14,46] They generally appear orange in color and exhibit very anisotropic linewidths. Our 0.1% samples showed a full width,

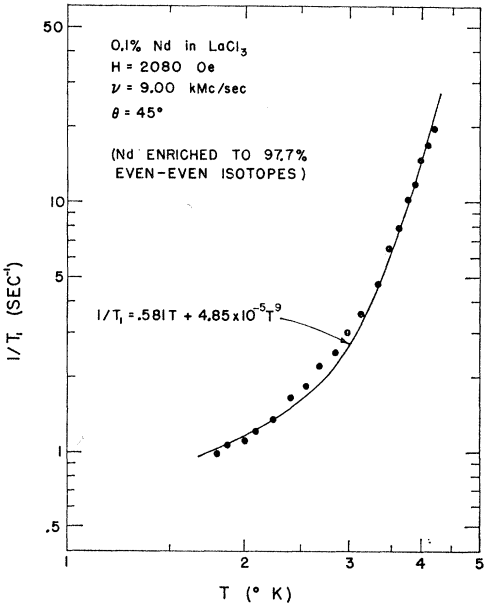

FIG. 8. Temperature dependence of the relaxation rate of 0.1% Nd^{3+} (97.7% enriched even-even) in $LaCl_3$ for $\theta=45°$.

[44] M. S. Magno and G. H. Dieke, J. Chem. Phys. **37**, 2354 (1962).
[45] J. D. Axe and G. H. Dieke, J. Chem. Phys. **37**, 2364 (1962).
[46] J. C. Eisenstein, R. P. Hudson, and B. W. Mangum, Phys. Rev. **137**, A1886 (1965).

half-maximum linewidth which varied from about 7 Oe at $\theta=0°$ to around 150 Oe at $\theta=90°$. The formation of Sm^{2+} seems to be the source of difficulty.[14]

The recovery of the Sm^{3+} resonance signal after saturation can be described by two exponential rates. The initial 25–75% of the signal recovered with a rate that was between two and one hundred times faster than the final portions, or tail, of the signal. This suggests spectral diffusion effects[47] which we confirmed by modulation of the magnetic field with simultaneous pulse saturation. It could then be observed that after the saturating pulse, a hole was present in the resonance line which quickly diffused throughout the line producing a slightly diminished but otherwise normally shaped resonance line which approached an equilibrium value at a much slower rate. It is this slower rate which we measured and consider to be the normal relaxation rate $1/T_1$.

The relaxation data at $\theta=0°$ for three samples containing 0.1% Sm^{3+} are presented in Fig. 9. All three show essentially the same Orbach and Raman rates but different direct process coefficients. The data can be fit to

$$1/T_1=AT+3.4\times10^{11}\exp(-58.6/T)+0.020T^9\ \text{sec}^{-1}, \quad (33)$$

where $A(S2A)=0.0347\pm0.014$ sec^{-1} $°\text{K}^{-1}$, $A(S2B)=3.34\pm0.17$ sec^{-1} $°\text{K}^{-1}$, and $A(S3)=0.854\pm0.091$ sec^{-1} $°\text{K}^{-1}$. The uncertainties in B and C' are $\pm0.09\times10^{11}$ sec^{-1} and ±0.001 sec^{-1} $°\text{K}^{-9}$, respectively. The apparent variation in the A coefficient with sample may only reflect the greater difficulty in measuring the final signal recovery rate at lower temperatures.

The relaxation calculations of Sm^{3+} are similar to those for Ce^{3+}. It is necessary to include a Zeeman admixture of the very distant states $|11\rangle$ and $|12\rangle$ of Table IV into the ground doublet in order to obtain a nonzero value of $A(\theta=0°)$.[10] The result is $A(0°)=0.47$ sec^{-1} $°\text{K}^{-1}$. We have calculated the theoretical angular dependence of the direct process under the assumption

TABLE IV. Experimental crystal field splittings[a] and calculated wave functions for the two lowest lying levels of Sm^{3+} ($4f^5$, $^6H_{5/2}$ and $^6H_{7/2}$) in $LaCl_3$. The wave functions are computed using the crystal field parameters listed in the text and are written in terms of $|J,J_z\rangle$.

n	E_n (cm^{-1})	Wave functions $\lvert n\rangle$ for $\theta=0°$
13,14	1172.6	$0.999(0.773\lvert\frac{7}{2},\pm\frac{5}{2}\rangle+0.635\lvert\frac{7}{2},\mp\frac{7}{2}\rangle)\mp0.042\lvert\frac{5}{2},\pm\frac{5}{2}\rangle$
11,12	1104.7	$0.998\lvert\frac{7}{2},\pm\frac{1}{2}\rangle\mp0.056\lvert\frac{5}{2},\pm\frac{1}{2}\rangle$
9,10	1051.2	$1.000(0.773\lvert\frac{7}{2},\pm\frac{5}{2}\rangle-0.635\lvert\frac{7}{2},\mp\frac{7}{2}\rangle)\pm0.013\lvert\frac{5}{2},\pm\frac{5}{2}\rangle$
7,8	992.8	$1.000\lvert\frac{7}{2},\pm\frac{3}{2}\rangle\mp0.009\lvert\frac{5}{2},\pm\frac{3}{2}\rangle$
5,6	66.1	$0.999\lvert\frac{5}{2},\pm\frac{5}{2}\rangle\pm(0.020\lvert\frac{7}{2},\pm\frac{5}{2}\rangle-0.036\lvert\frac{7}{2},\mp\frac{7}{2}\rangle)$
3,4	40.7	$1.000\lvert\frac{5}{2},\pm\frac{3}{2}\rangle\pm0.009\lvert\frac{7}{2},\pm\frac{3}{2}\rangle$
1,2	0.0	$0.998\lvert\frac{5}{2},\pm\frac{1}{2}\rangle\pm0.056\lvert\frac{7}{2},\pm\frac{1}{2}\rangle$

[a] See Ref. 45.

[47] W. B. Mims, K. Nassau, and J. D. McGee, Phys. Rev. **123**, 2059 (1961).

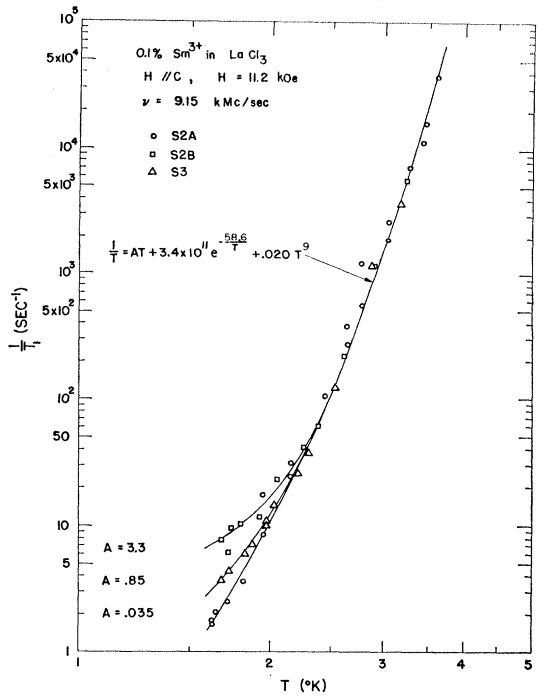

FIG. 9. Relaxation data for three samples of $LaCl_3$ containing 0.1% Sm^{3+}. Samples S2A and S2B are from different portions of the same melt.

that the contributions to $A(\theta)$ from the distant (≥990 cm^{-1}) states $|7\rangle$ through $|14\rangle$ is constant and equal to the contribution at $\theta=0°$. At other angles, Zeeman admixtures are calculated using only the nearly (≤67 cm^{-1}) states $|1\rangle$ through $|6\rangle$. For these six states the contribution at $\theta=0°$ is zero and at $\theta=90°$ it is 12.75 sec^{-1} $°\text{K}^{-1}$.

In Fig. 10 we have drawn a solid line corresponding to 2.25 times the theoretical $A(\theta)$ so that a comparison can be made with the experimental values measured for sample $S3$ assuming an isotropic Orbach and Raman process. Aside from the factor of 2.25, the agreement is quite good. The theoretical values for the Orbach and Raman coefficients at $\theta=0°$ are $B=2.24\times10^{10}$ sec^{-1} and $C'=0.12\times10^{-3}$ sec^{-1} $°\text{K}^{-9}$, if admixtures from the $J=7/2$ level are neglected.

E. Terbium, $4f^8$

The optically determined[48] crystal-field splittings of the $^7F_6$ ground level of Tb^{3+} in $LaCl_3$ are listed in Table V. Also included are the calculated wave functions using the crystal field parameters[48] $A_2{}^0\langle r^2\rangle=92$ cm^{-1}, $A_4{}^0\langle r^4\rangle=-40$ cm^{-1}, $A_6{}^0\langle r^6\rangle=-30$ cm^{-1}, and $A_6{}^6\langle r^6\rangle=290$ cm^{-1}. Magnetic resonance is observed between the two lowest states which are separated by 0.2 cm^{-1} due to the static crystal field. It is important

[48] K. S. Thomas, S. Singh, and G. H. Dieke, J. Chem. Phys. **38**, 2180 (1963).

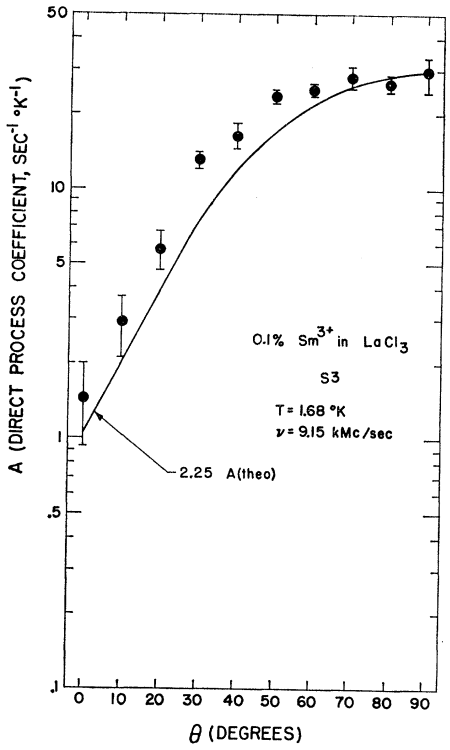

FIG. 10. Angular dependence of the direct process coefficient $A(\theta)$ of sample S3 containing 0.1% Sm^{3+} in $LaCl_3$. The solid line is 2.25 times the theoretical expression for $A(\theta)$ as derived using the approximation noted in the text.

to note that this quasidoublet has a splitting which is independent of any random deviations from C_{3h} symmetry which are usually invoked to account for the observed resonance in a non-Kramers' ion.[39] Consequently Tb^{3+} is characterized by a line-shape and a direct-process relaxation rate which is more in accord with Kramers ions.

The paramagnetic resonance spectrum of Tb^{159} (100% abundant) consists of four hyperfine lines described by[14] $g_{11}=17.17\pm0.01$, $A=0.212\pm0.003$ cm^{-1}, $\Delta=0.201$ cm^{-1}, $S=1/2$, and $I=3/2$. At X-band frequencies the two lowest field hyperfine lines overlap while the two higher field lines are well resolved and show a full-width half-maximum linewidth which varies from 8 Oe at $\theta=0°$ to about 47 Oe at 75°. The angular dependence is well described by the assumption of small local lattice distortions.[49] The relaxation data presented here correspond to measurements of the two higher field hyperfine lines for which the signal recoveries involved a single exponential. Measurements taken on the overlapping lower lines indicated nonexponential recoveries.

In the parallel orientation, all data for both 1% and 0.1% Tb^{3+} in $LaCl_3$ could be fit to the curve of Fig. 11:

$$1/T_1=4.26T+4.83\times10^{11}\exp(-81.8/T)+0.027T^7 \text{ sec}^{-1}. \quad (34)$$

The probable errors in the coefficients of the direct, Orbach, and Raman processes are ±0.15 sec^{-1} °K^{-1}, $\pm0.02\times10^{11}$ sec^{-1}, and ±0.001 sec^{-1} °K^{-7}, respectively. A least-squares fit to Δ_3 yielded 84.1 ± 5°K. Within experimental error, the Orbach and Raman rates did not display any angular dependence and agreed within a factor of 4 with the theoretically predicted values of 1.18×10^{11} sec^{-1} and 0.0065 sec^{-1} °K^{-7}.

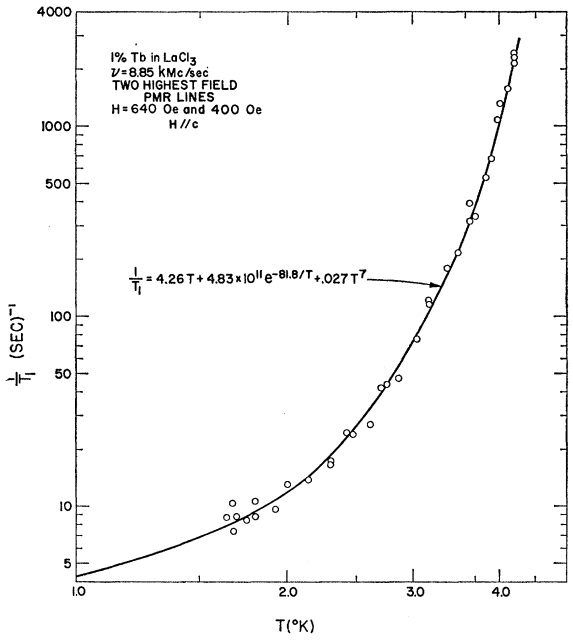

FIG. 11. Relaxation data for 1% Tb^{3+} ($I=\frac{3}{2}$) in $LaCl_3$ at 8.85 kMc/sec with the magnetic field parallel to the crystal axis. The data represent measurements taken for the two highest field hyperfine lines. Data taken on a sample containing 0.1% Tb^{3+} are not shown but also fit this same temperature dependence. (PMR = paramagnetic resonance).

TABLE V. Experimental crystal field splittings[a] and calculated wave functions for the ground level of Tb^{3+} ($4f^8$, $^7F_6$) in $LaCl_3$. The wave functions are computed using the crystal field parameters listed in the text and are written in terms of $|J_z\rangle$ with $J=6$.

n	E_n (cm^{-1})	Wave functions $\|n\rangle$ for $\theta=0°$
13	117.99	$0.707\|3\rangle-0.707\|-3\rangle$
11, 12	112.80	$0.805\|\pm2\rangle-0.593\|\mp4\rangle$
10	104.64	$0.707\|3\rangle+0.707\|-3\rangle$
8, 9	99.31	$0.805\|\pm4\rangle+0.593\|\mp2\rangle$
6, 7	97.22	$0.986\|\pm1\rangle-0.169\|\mp5\rangle$
5	90.56	$0.998\|0\rangle-0.040(\|6\rangle+\|-6\rangle)$
3, 4	56.83	$0.986\|\pm5\rangle+0.169\|\mp1\rangle$
2	0.20	$0.707\|6\rangle-0.707\|-6\rangle$
1	0.00	$0.706(\|6\rangle+\|-6\rangle)+0.056\|0\rangle$

[a] See Ref. 48.

Figure 12 shows the angular dependence of the direct process coefficient $A(\theta)$ for Tb^{3+}. It is interesting for two reasons: (1) the magnitude of $A(\theta)$ is very small for a non-Kramers ion (compare with Pr^{3+}), and (2)

[49] P. L. Scott, H. J. Stapleton, and C. Wainstein, Phys. Rev. 137, A71 (1965).

the angular variation rises sharply for $\theta \geq 50°$. Since $g_\perp$ is identically zero, the only way an anisotropy can enter the calculations for $A(\theta)$ is through the Zeeman admixture of excited state wave functions into the ground doublet $|a\rangle$ and $|b\rangle$ to form $|1'\rangle$ and $|2'\rangle$. It is worth while examining the various contributions to $A(\theta)$ in some detail. The isotropic term $|\langle a|V_c|b\rangle|^2$ is nonzero only by virtue of the antisymmetric V_6^{-6} operator. It contributes a constant amount 1.01 sec^{-1} $°\text{K}^{-1}$ to $A(\theta)$. The Zeeman admixture at 9.17 kMc/sec varies from 6×10^{-6} sec^{-1} $°\text{K}^{-1}$ at $\theta=0°$ due to an admixing of state $|5\rangle$ to 3.4 sec^{-1} $°\text{K}^{-1}$ at $\theta=80°$ due to mixing from states $|3\rangle$ through $|7\rangle$. As in the case of the terbium Raman and Orbach processes, the theoretical direct process rate appears to be about 1/4 of the experimental rate. In Fig. 12 the theoretical values of $4A(\theta)$ are compared with experiment with remarkable agreement.

F. Erbium, $4f^{11}$

The $^4I_{15/2}$ ground level of Er^{3+} is well separated ($\approx$6480 cm^{-1}) from the first excited J manifold. Table VI lists the optically determined[50] crystal-field splittings of the $J=15/2$ level and the calculated wave functions using the static crystal-field parameters $A_2{}^0\langle r^2\rangle=93.89$ cm^{-1}, $A_4{}^0\langle r^4\rangle=-37.28$ cm^{-1}, $A_6{}^0\langle r^6\rangle=-26.56$ cm^{-1}, and $A_6{}^6\langle r^6\rangle=265.2$ cm^{-1}. Except for Er^{167} which is 22.9% abundant, the isotopes of naturally occurring erbium are even-even. The paramagnetic resonance spectrum for the even-even isotopes is described[14] by $g_{11}=1.989\pm0.001$, $g_\perp=8.757\pm0.002$, and $S=1/2$. Er^{167} requires in addition $I=7/2$, $A=(6.64\pm0.03)\times10^{-3}$ cm^{-1}, $B=(3.04\pm0.02)\times10^{-2}$ cm^{-1}, and $P=8.6\times10^{-4}$ cm^{-1}. The strong central resonance due to the even-even isotopes overlaps one of the hyperfine lines of the Er^{167} spectrum. All measurements on the relaxation behavior of the central PMR line in samples doped with naturally abundant erbium exhibited a non-exponential concentration-dependent behavior. In addition the relaxation rate measured in the tails of these recoveries could not be fit to any of the usual temperature dependencies. To avoid these complications the measurements reported in this paper were taken from samples doped with enriched (97.9% even-even) isotopes of erbium. For these samples the relaxation signals involved essentially a single exponential rate over the last 50% of the recovery. For all of the erbium doped samples we grew, containing either enriched and natural isotopes, the main resonance line showed structure. It was about 3.3-Oe wide at $\theta=90°$ and became a broad ($\approx$55 Oe) multipeaked resonance at $\theta=0°$. Since pure $ErCl_3$ is monoclinic[51] rather than hexagonal, these resonance line-shape effects may be unavoidable in the mixed crystal.

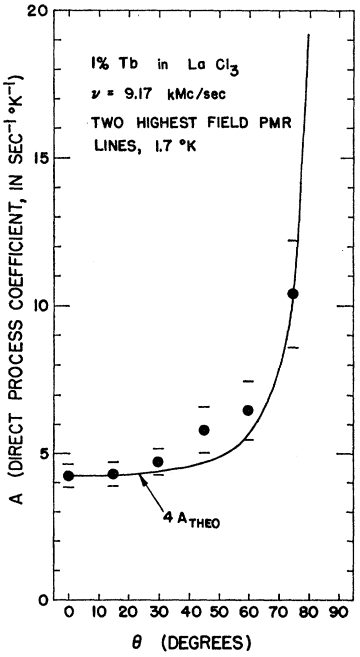

FIG. 12. Angular dependence of the direct process coefficient $A(\theta)$ for $LaCl_3$ containing 1% Tb^{3+}. The solid curve represents four times the calculated value of $A(\theta)$.

TABLE VI. Experimental crystal field splittings[a] and calculated wave functions for the ground level of Er^{3+} ($4f^{11}$, $^4I_{15/2}$) in $LaCl_3$. The wave functions are computed using the crystal field parameters listed in the text and are written in terms of $|J_z\rangle$ with $J=15/2$.

n	E_n (cm^{-1})	Wave functions $\|n\rangle$ at $\theta=0°$
15, 16	229.31	$0.876\|\pm\frac{13}{2}\rangle+0.401\|\pm\frac{1}{2}\rangle+0.268\|\mp\frac{11}{2}\rangle$
13, 14	181.04	$0.789\|\pm\frac{11}{2}\rangle+0.431\|\mp\frac{1}{2}\rangle-0.439\|\mp\frac{13}{2}\rangle$
11, 12	141.61	$0.103\|\pm\frac{15}{2}\rangle+0.778\|\pm\frac{3}{2}\rangle+0.620\|\mp\frac{9}{2}\rangle$
9, 10	113.70	$0.657\|\pm\frac{7}{2}\rangle+0.754\|\mp\frac{5}{2}\rangle$
7, 8	96.52	$0.201\|\pm\frac{13}{2}\rangle-0.808\|\pm\frac{1}{2}\rangle$
5, 6	64.72	$0.829\|\pm\frac{15}{2}\rangle+0.277\|\pm\frac{3}{2}\rangle-0.486\|\mp\frac{9}{2}\rangle$
3, 4	37.91	$0.550\|\pm\frac{15}{2}\rangle-0.564\|\pm\frac{3}{2}\rangle+0.616\|\mp\frac{9}{2}\rangle$
1, 2	0.00	$0.754\|\pm\frac{7}{2}\rangle-0.657\|\mp\frac{5}{2}\rangle$

[a] See Ref. 50.

The temperature dependence of the relaxation of 1% enriched Er^{3+} in $LaCl_3$ is shown in Fig. 13 for the magnetic field perpendicular to the crystal axis. These data fit

$$1/T_1=2.26T+1.14\times10^{10}\exp(-54.6/T)+3.46\times10^{-3}T^9\ \text{sec}^{-1}, \quad (35)$$

where the uncertainties in A, B, and C' are ±0.06 sec^{-1} $°\text{K}^{-1}$, $\pm0.05\times10^{10}$ sec^{-1}, and $\pm0.2\times10^{-3}$ sec^{-1} $°\text{K}^{-9}$, respectively. The theoretical values of A, B, and C' computed for $\theta=90°$ are: $A=2.73$ sec^{-1} $°\text{K}^{-1}$, $B=1.66\times10^{10}$ sec^{-1}, and $C'=0.679\times10^{-3}$ sec^{-1} $°\text{K}^{-9}$. The theoretical expressions for B and C' change by only 6% and 10%, respectively, between $\theta=0°$ and 90°, but the total theoretical relaxation rate $1/T_1$ at 2.84°K changes by only 3% between parallel and perpendicular orientations. Figure 14 shows the experimental and calculated relaxation rates between 0° and 90° at 2.84

[50] J. C. Eisenstein, J. Chem. Phys. **39**, 2128 (1963).

[51] R. W. Wykoff, *Crystal Structures* (Interscience Publishers, Inc., New York, 1957), Vol. II, Chap. V, p. 64.

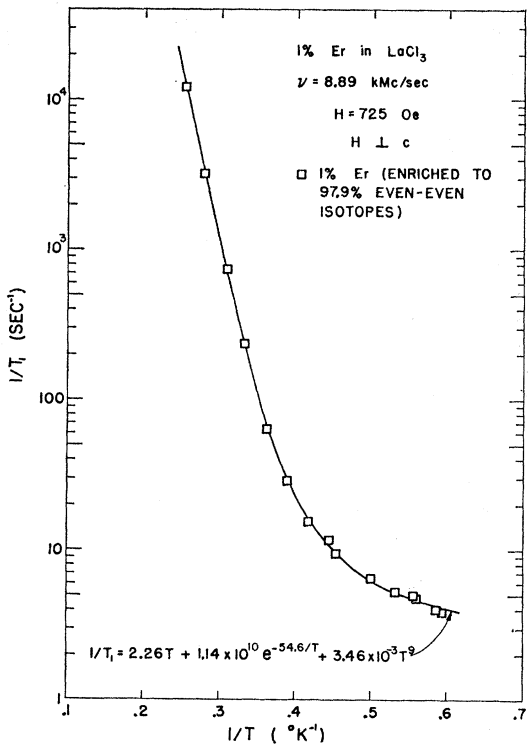

FIG. 13. Relaxation data for 1% Er^{3+} (97.9% enriched even-even) in $LaCl_3$ at 8.89 kMc/sec with the magnetic field perpendicular to the crystal axis.

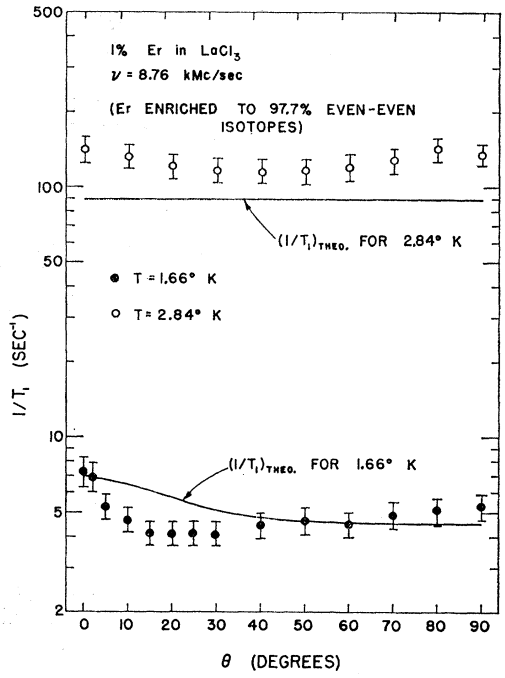

FIG. 14. Angular dependence of the total relaxation rate $1/T_1$ of 1% Er^{3+} (97.9% enriched even-even) in $LaCl_3$ at 8.76 kMc/sec for 1.66 and 2.84°K. The solid curves represent the theoretically predicted relaxation anisotropy at these same two temperatures.

and 1.66°K. At the lower temperature the direct process is dominant and both the experimental and theoretical relaxation rates show a very weak anisotropy. While the observed and calculated rates are in somewhat better agreement than usual, the observed weak anisotropy does not follow the predicted form as closely as one might expect. This could be related to the observed structure on the erbium resonance line or to cross relaxation effects with a cerium impurity, which would cross the erbium resonance at $\theta=22°$. The latter seems unlikely however since the erbium rate is slowest at that angle and both ions have comparable relaxation times.

V. SUMMARY

The over-all agreement between our measured and calculated relaxation rates for cerium, praseodymium, neodymium, samarium, terbium, and erbium in lanthanum trichloride is quite satisfactory except for cerium. A review of the agreement for the direct process coefficient yields the following typical error factors: 80 for Ce(0°), 2 for Nd(45°), 2 for Sm ($S3$ at 0°), 4 for Tb(0°), and 1.2 for Er(90°). A similar survey of the Orbach coefficients B yields: 100 for Ce, 13 for Pr, 15 for Sm (neglecting admixtures from the excited $J=7/2$ level), 4 for Tb, and 1.5 for Er. Finally the Raman coefficients agree within factors of: 1.3 for Nd, 170 for Sm (again neglecting $J=7/2$ admixtures), 4 for Tb, and 5 for Er. It should be noted that the theoretical values were low about 70% of the time. The worst agreement is for cerium for which no optical data were available to determine the static crystal field parameters.

As far as the angular anisotropy of T_1 is concerned, the predicted form is in remarkable agreement with experiment for every case where a significant anisotropy is observed. In the theoretical approach to this problem it is particularly interesting to note the importance of matrix elements connecting excited states with the ground doublet through the Zeeman interaction.

Finally the existence of a predicted phonon bottleneck in the direct process relaxation of Pr^{3+} is gratifying. The apparent short equilibration time ($\approx$80 nsec) and its change after neutron bombardment are both puzzling effects and more detailed experiments are planned. For the sake of completeness we present here the results of our theoretical calculations for holmium which we were unable to measure because of poor signal strength. Our calculations for $\theta=0°$ yield: $A=1.86\times10^5$ sec^{-1} °K^{-1}, $B=1.08\times10^{10}$ sec^{-1}, and $C+C''=2.15\times10^2$ sec^{-1} °K^{-7}. In spite of the fact that the first excited state is removed by only 18°K,[52] the predominant process at 1°K is the direct mechanism with a resultant relaxation time of about 5 μsec if a bottleneck is ignored. On the basis of these calculations and our results for Pr^{3+}, we believe that the direct-process relaxation of trivalent holmium is severely bottlenecked in the trichloride.

[52] G. H. Dieke and B. Pandey, J. Chem. Phys. 41, 1952 (1964).